ANNUAL PROGRESS REPORT ON STUDIES OF MICROWAVE SCATTERING AND CANOPY ARCHITECTURE FOR BOREAL FORESTS

G. Lance Lockhart and S. P. Gogineni

Radar Systems and Remote Sensing Laboratory
Department of Electrical Engineering and Computer Science, University of Kansas
2291 Irving Hill Road, Lawrence, Kansas 66045-2969
TEL: 913/864-4835 * FAX: 913/864-7789 * E-MAIL: graham@ardneh.rsl.ukans.edu

RSL Technical Report 10480-3

August 1995

Sponsored by:

NASA Goddard Space Flight Center
Greenbelt MD 20771

Grant NAG 5-2344

1.0 Introduction

This is an annual report on the project titled "Study of Microwave Scattering and Canopy Architecture for Boreal Forests." The objectives of our work are to study the interaction of microwave signals with vegetation components and to determine the radar's ability to provide accurate estimates of biophysical parameters such as biomass. Our research is aimed at refining the current microwave models and using these improvements to facilitate more accurate interpretations of SAR imagery.

During the summer of 1994, we participated in IFC-2 and collected scatterometer data at C and X bands in the southern study area (SSA). The sites where we collected data included the young jack pine (YJP), the old jack pine (OJP), the old black spruce (OBS), and the old aspen (OA). We experienced some system problems during IFC-2, and we devised a plan to repair these problems for IFC-3. As a complement to the helicopter-based scatterometer data, we collected ground reflectance data at the OJP site using a network-analyzer-based step-frequency radar.

When we returned from IFC-2, we made improvements to the radar and built a new L-band radar for use in IFC-3. The improvements that we made to the radar system during this time include the replacement of the IF amplifiers, the construction of a new control box with a lightweight power supply and an incidence angle readout, and the improvement of the data acquisition software to provide faster write times and better synchronization.

We returned to the SSA for IFC-3 and performed helicopter-based scatterometer measurements over the IFC-2 sites. The radar performed much better but we still had some grounding problems. We felt that we needed either more transmit power or more amplifier gain. Therefore, we resolved to repackage the radar and take care of any grounding problems and to add 30 dB gain to our C- and X-band IF amplifiers.

After IFC-3, we spent the next semester repackaging the radar and adding another gain level to the IF amplifiers. We also began processing data from the YJP site taken during IFC-3. Several power return versus range plots were created to illustrate the radar's ability to determine the scattering from various canopy components relative to the total scattering from the forest. In addition, a program was developed to calculate the scattering coefficient of the forest as a function of incidence angle.

To evaluate the performance of the radar after the improvements were made to the system, with the help of Dr. Jon Ranson, we conducted an experiment in June 1995 at the NASA-Wallops Flight Facility (WFF). Flight lines were set up and several stands were identified as candidates for study. We flew four

lines covering a total of eight stands. The stands ranged from conifer to deciduous and from thick understory to little or no understory.

The experiment at WFF was successful and we collected a large quantity of data at L, C and X bands. Currently, these data are being processed and a plan has been developed to relate the scattering from various layers within the forest to the biomass within these layers.

2.0 Helicopter-Based Scatterometer Measurements During IFC-3

2.1 Improvements to the Radar System

During the time between IFC-2 and IFC-3, we made several improvements to the radar system. First, we built a new L-band scatterometer that will mount on the outside of the helicopter along with the log-periodic feeds. By placing the L-band scatterometer with the feeds, we eliminated the problems associated with using long cables between the RF section output and the feed antenna input.

Also, a new control box was built in an effort to decrease the weight of the system and to provide easier access to the radar output channels during the flights. Figure 1 shows the control box that was constructed.

New IF amplifiers were also added to the system. The new amplifiers provide three digitally controlled gain stages. The new amplifiers also have the ability to drive the 50-Ω load at the input to the A/D board.

During IFC-2, we were not getting the isolation performance from the RF switch that we were getting in the laboratory. When we were on the helicopter, we noticed that the switch driver circuit was becoming very hot. To solve this problem, we designed a more robust circuit and replaced the old circuit. After IFC-2, we put this circuit on a printed circuit board and installed it permanently in the RF box.

Another problem that we encountered during IFC-2 was that the time to transfer data from RAM to the hard disk was prohibitively large. We modified the data acquisition program and decreased the write time by a factor of two. We also made other improvements to the data acquisition program that would allow us to monitor the return signals during the flight.

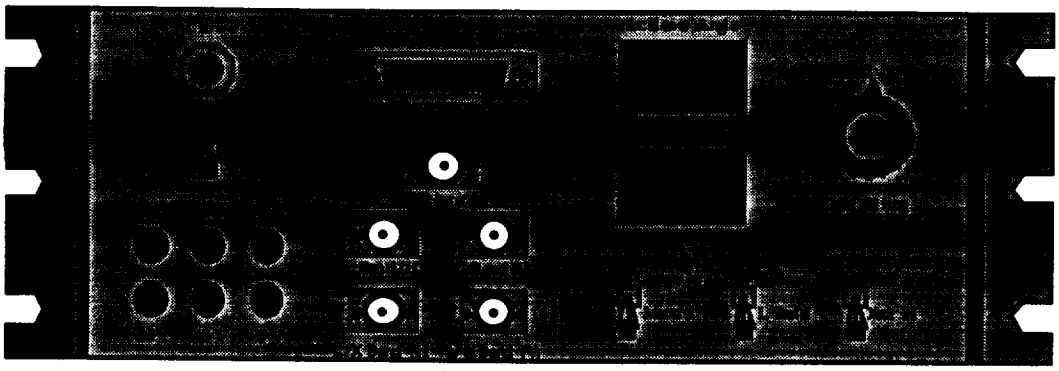

Front Panel

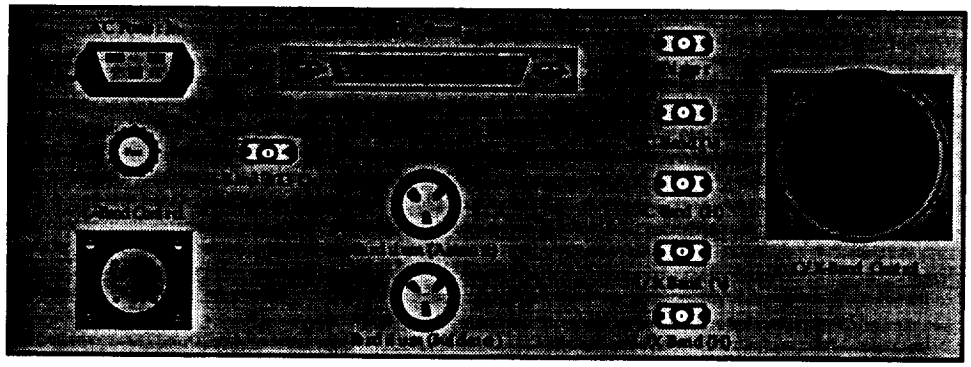

Back Panel

Figure 1. Front and back panel of radar control box

2.2 Data Collected During IFC-3

During IFC-3, we flew over four main flight lines. These included two lines at YJP (which includes OJP), one line at OBS, and one line at OA. The YJP lines are designated as either Alligator or non-Alligator in reference to the alligator-shaped stand near the line. Each of the flight lines is 800 meters long and we flew at a speed of 40 knots, which corresponds to roughly 20 meters/second. The flight lines were marked with orange forestry flags or by an easy-to-find landmark. We attempted to keep an altitude of 150 feet (46 meters) during all of the flights. The lines were flown multiple times to facilitate the collection of data at several different incidence angles. Table 1 is a detailed listing of all the data collected during IFC-3. Some of the data sets include just one angle with varying altitude. These data are used to provide an indication of whether or not we were flying at the proper altitude.

Table 1. Scatterometer data taken during IFC-3

Flight Number	Site Code	Incidence	Polarizations
1(9/14/94)	YJP(non-alligator line)	5°,10°,15°,20° 30°,40°,50°	VV,HH,VH and HV
1(9/14/94)	YJP(non-alligator line)	5°	HH and HV
1(9/14/94)	YJP(alligator line)	5°,10°,20°,30°40°,50°	VV,HH,VH and HV
1(9/14/94)	OBS (OS)	5°,10°,20°,30°40°,50°	VV,HH,VH and HV
2(9/15/94) h = 110 ft	OA (Old Aspen)	5°,10°,20°,30° 40°,50°	VV,HH,VH and HV
2(9/15/94) h = 110 ft	OBS (OS)	5°	VV,HH,VH and HV
2(9/15/94) h = 170 ft	OBS (OS)	5°	VV,HH,VH and HV
2(9/15/94)	OBS (OS)	10°,20°,30°, 40°,50°	VV,HH,VH and HV
3(9/16/94)	YJP (non-alligator line)	5°,10°,20°,30°40°,50°	VV,HH,VH and HV
3(9/16/94)	YJP (non-alligator line)	30°	VV and VH
3(9/16/94)	YJP (alligator line)	5°,10°,20°,30° 40°	VV,HH,VH and HV
3(9/16/94)	YJP (alligator line)	5°,10°,20°,30°	VV,HH,VH and HV

3.0 Results of IFC-3 Data

The scattering coefficient (σ^o) versus incidence angle for L-band HH measurements over the YJP site is shown in figure 2. We used eight samples for each of the angles to reduce the variance of the scattering coefficient estimate. A third-order polynomial fit to the data is also shown.

Figure 2 shows a 15-dB decrease in backscattering coefficient as the incidence angle increases from 5° to 20°. This decrease in scattering coefficient indicates that surface scattering from the forest floor is dominant at lower incidence angles. As the incidence angle increases, volume scattering becomes dominant and the slope of the scattering coefficient curve decreases.

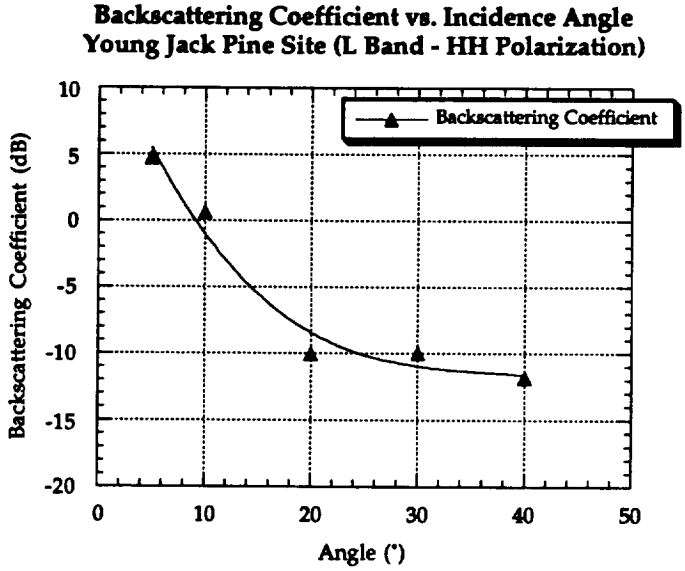

Figure 2. Backscattering coefficient versus angle for YJP (L band)

Figure 3 is a comparison of the L-band HH return at incidence angles of 5° and 30°. These two plots show the general trend of the L-band data collected over the YJP site. At 5°, the dominant return is that of the ground, and at 30°, the return has spread out over more range cells and no single return is dominant.

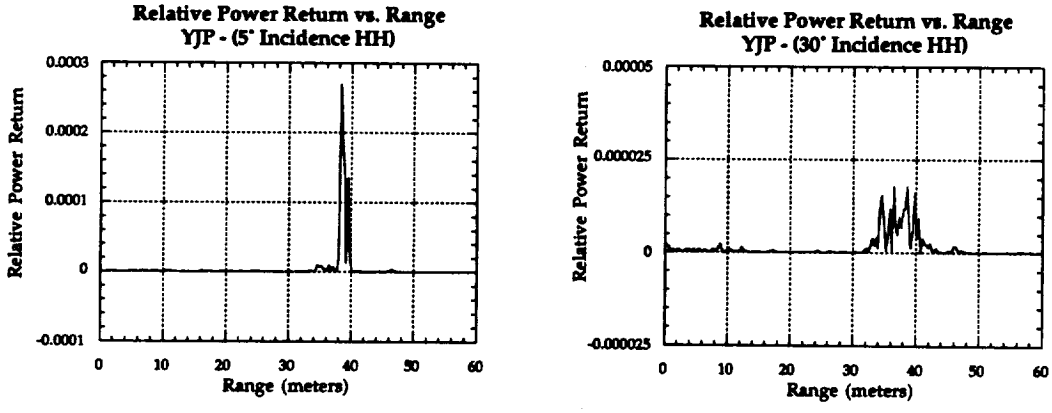

Figure 3. Power return vs. range for YJP (L band)

The C-band backscattering coefficient as a function of incidence angle is plotted in figure 4. The 3-dB decrease in backscattering coefficient as incidence angle increases from 5° to 20° is substantially less than the 15-dB decrease shown in figure 2.

At C band the ground can still be seen at lower incidence angles. However, the percentage of the signal reflected by the ground is lower at C band than at L band. Therefore, we see a more gradual decrease in the scattering coefficient as the incidence angle increases. This is evident in figure 5, which shows the relative power returned versus range for a typical 5° and 30° return at C band over the YJP site.

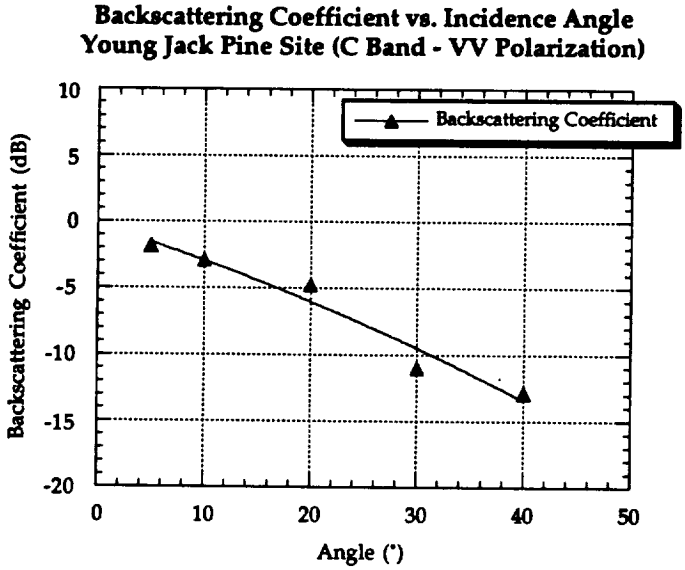

Figure 4. Backscattering coefficient versus angle for YJP (C band)

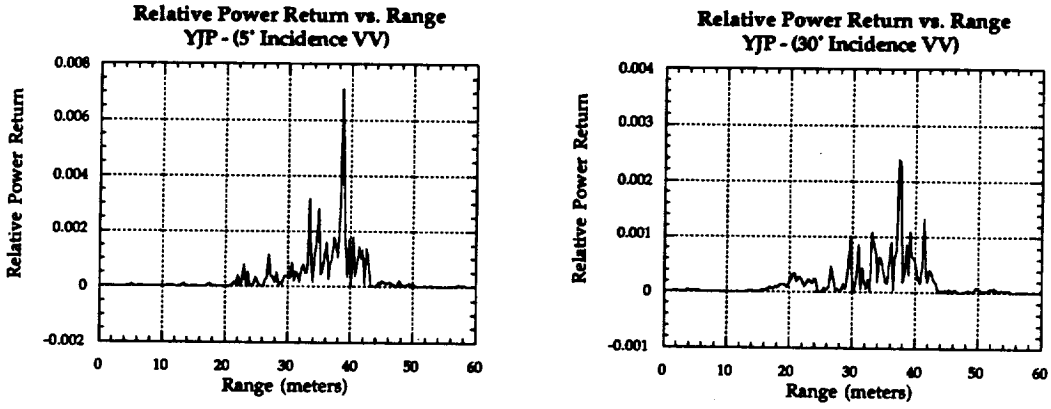

Figure 5. Power return vs. range for YJP (C band)

3.1 Calibration

We did not perform external calibration in the field due to the difficulties in locating the calibration target from the helicopter. However, external calibration was performed at The University of Kansas upon returning from the field. For the purposes of this paper, we have cross calibrated the data using AIRSAR results [1].

4.0 Improvements to the Radar System after the 1994 Campaigns

Although the radar performed well during IFC-3, we decided that further improvements should be made. Several times throughout the course of the summer experiments we needed access to the RF section. However, the RF section was mounted on the rack in the helicopter and it was not easy to access. Therefore, we designed a new box for the radar with a plate that slides in and out for easy access to the RF section during field experiments. Figure 6 is an illustration of the box and the layout of the radar components within the box. In addition to repackaging the RF section, we rewired all of the power and control signals.

The new RF box also provides housing for the new IF amplifiers. The new IF amplifiers are three-stage variable-gain amplifiers that have an area of about four square inches. Each of the six radar receive channels have a separate IF amplifier. The C- and X-band amplifiers are housed in a four-chamber box next to the RF sections. This box provides shielding between the amplifiers and improves the isolation between receive channels. The L-band amplifiers were also replaced, but they are not in a shielded box.

The new C- and X-band amplifiers include gains of 50, 70, and 90 dB. We went through several design iterations before we were able to implement successfully a 90-dB gain stage. At first, the amplifier was oscillating at the highest gain. Therefore, we suspected that there was a feedback loop that was causing these oscillations. After experimenting, we found that the feedback path was through the power supplies, and we placed inductors in the power supply path to reduce the amount of feedback. At present, we have achieved a gain of 90 dB with an isolation of more than 25 dB between channels. Therefore, the isolation is limited by the antennas, which have an isolation of about 20 dB, rather than by the amplifiers.

We also purchased high-quality RF cables from QMI, Incorporated for interconnecting the C- and X-band RF sections to the feed antennas. By using these low-loss cables, we effectively obtain a higher transmit power.

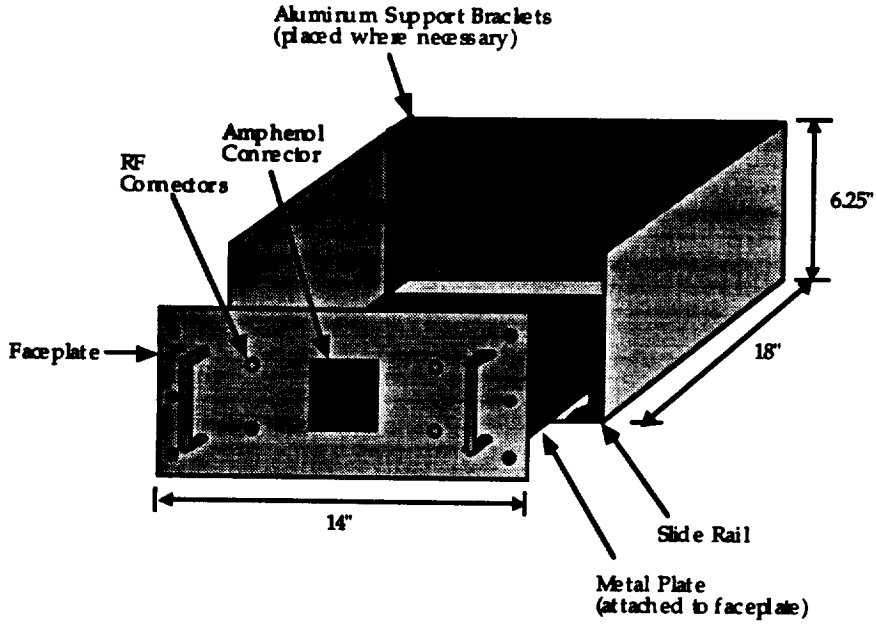

Three-Dimensional View of the Entire RF Box

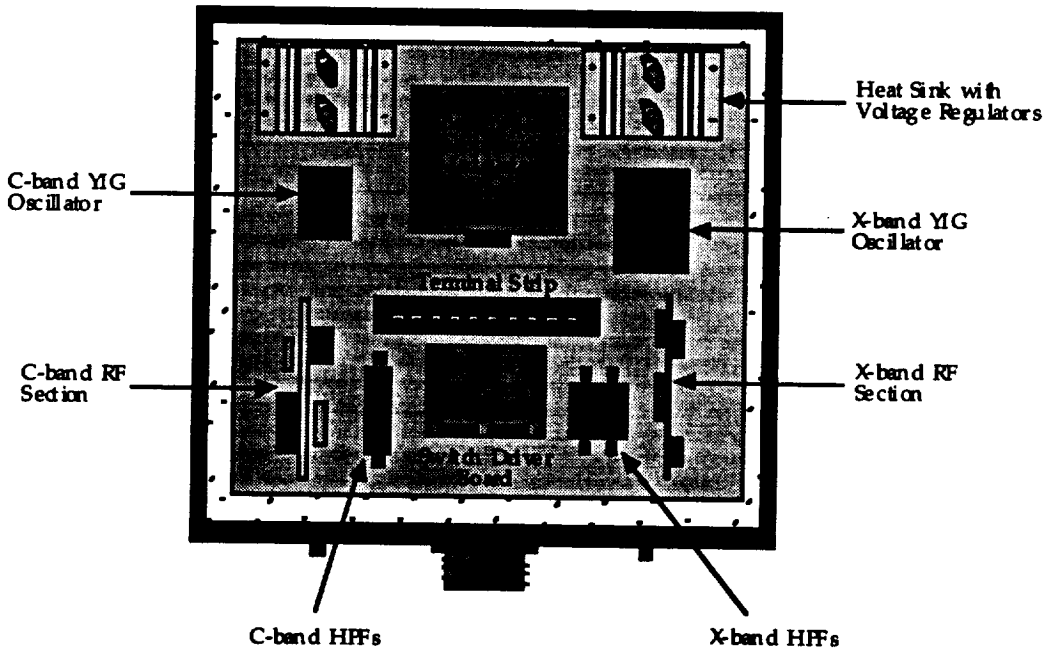

Top View of New RF Box Showing Component Layout

Figure 6. Drawing of new RF box

4.1 Antenna Pattern Measurements

During June 1995, we used the outdoor antenna range at NASA-GSFC to characterize the radar antenna. We were able to measure all of the patterns for the L-band antenna but we did not have a large enough signal level to measure the full patterns at C band and X band. However, at C band we were able to measure the main lobe. Figure 7 shows the azimuth and elevation cut for the L-band VV and VH patterns. Table 2 presents a summary of the important parameters for the L-band antenna.

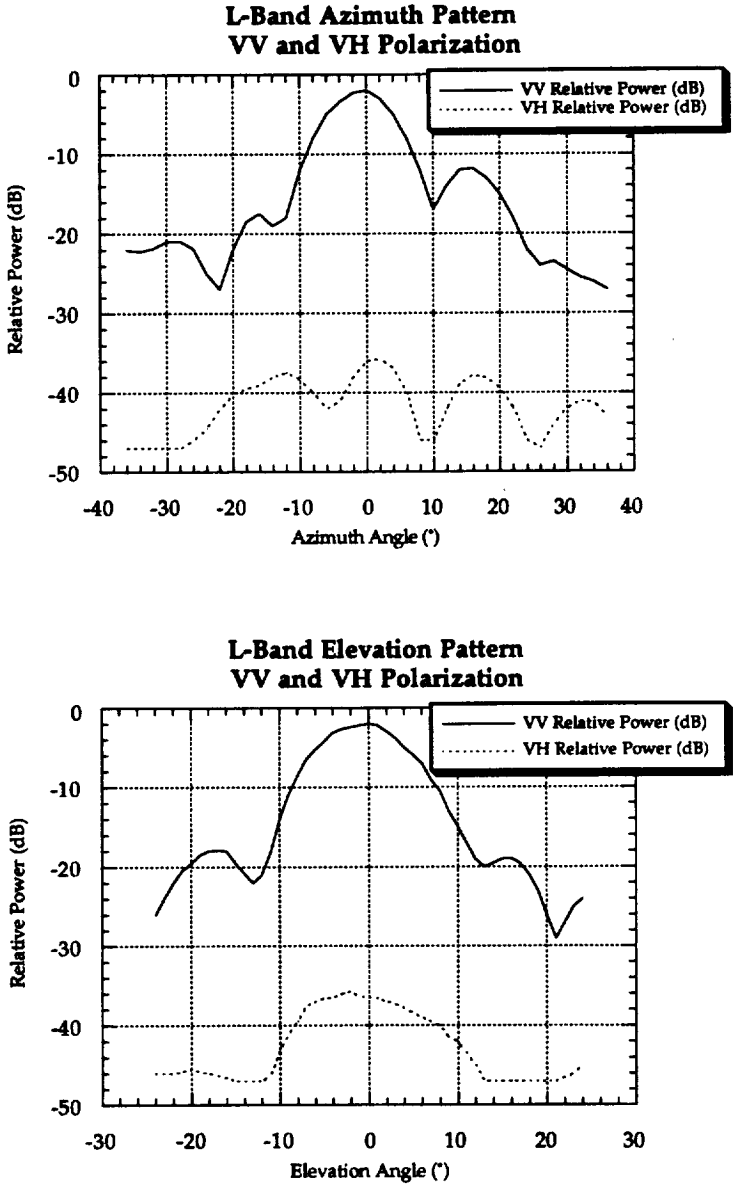

Figure 7. Azimuth and elevation cuts of L-band VV and VH patterns

Table 2. L-band antenna parameters

Frequency (GHz)	Plane	Polarization	3-dB Beamwidth	First Sidelobe Level (dB)	Minimum Isolation (dB)
2.0	Azimuth	VV	10°	10	N/A
2.0	Elevation	VV	10°	16	N/A
2.0	Azimuth	VH	8°	N/A	34 (VV)
2.0	Elevation	VH	14°	N/A	34 (VV)
2.0	Azimuth	HH	11°	11	N/A
2.0	Elevation	HH	11°	6	N/A
2.0	Azimuth	HV	10°	N/A	24 (HH)
2.0	Elevation	HV	20°	N/A	29 (HH)

5.0 Wallops Experiment

We conducted an experiment in June 1995 at NASA-WFF to test the improvements that we made to the radar. With the help of Dr. Jon Ranson and Dr. Roger Lang, we chose four flight lines over eight stands of trees. The flight lines varied in length between 400 meters and 600 meters. We flew each line at an altitude of 150 feet (46 meters) and a speed of 40 knots (20 meters/second) as in the BOREAS experiments. We boresighted a video camera with the L-band V antenna so that we could record the location of the radar's beam.

The stands consisted of both deciduous trees and conifers. The first stand on line one is loblolly pine with little understory and the second stand on line one is loblolly pine with a holly understory. The first stand on line three is older deciduous with little understory and the second stand is mixed conifer and deciduous. The primary stand on line four is a younger deciduous stand with very little understory. All of the stands mentioned above were measured using a technique developed by Dr. Jon Ranson's group. The measurements taken include species type, diameter at breast height (DBH), tree location, and tree height. These data will be used in conjunction with allometric formulas to determine the biomass of the various canopy components.

The radar performed well during this experiment with the exception of the L-band VV and HV channels. Therefore, for each of the four lines we have data from ten radar channels which include CVV, CVH, CHH, CHV, XVV, XVH, XHH, XHV, LHH, and LVH. We measured all of these channels at incidence angles of 5°, 25°, and 45°. Figures 8, 9, and 10 are relative power return versus range curves for L, C, and X bands, respectively. In figure 9, the first peak at approximately 36 meters is the top of the trees and the peak at 48 meters is the ground. These returns show the radar's ability to see both the top and bottom of the canopy at C band. Using this type of data, we can

determine the amount of scattering from various forest components at the various frequencies, polarizations, and angles of incidence.

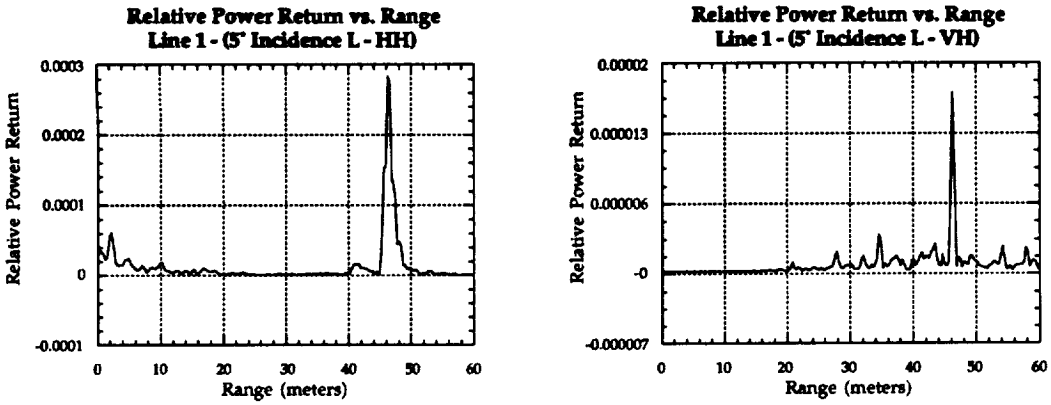

Figure 8. L-band returns from Wallops experiment

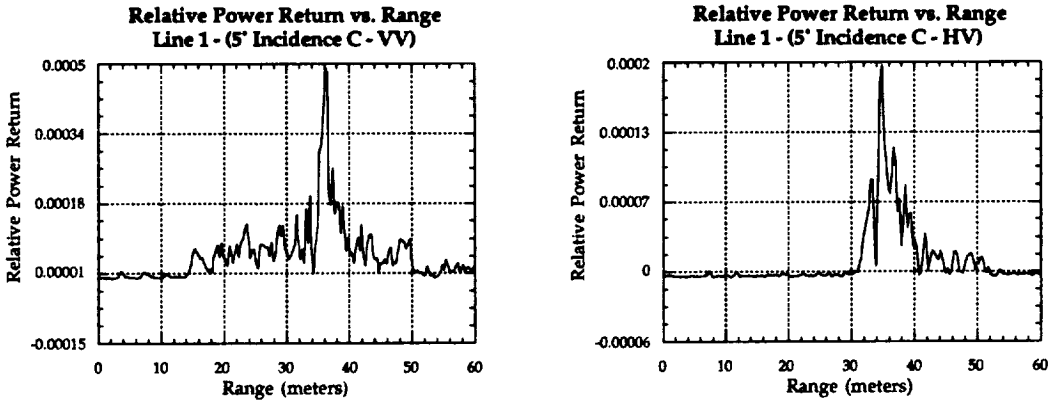

Figure 9. C-band returns from Wallops experiment

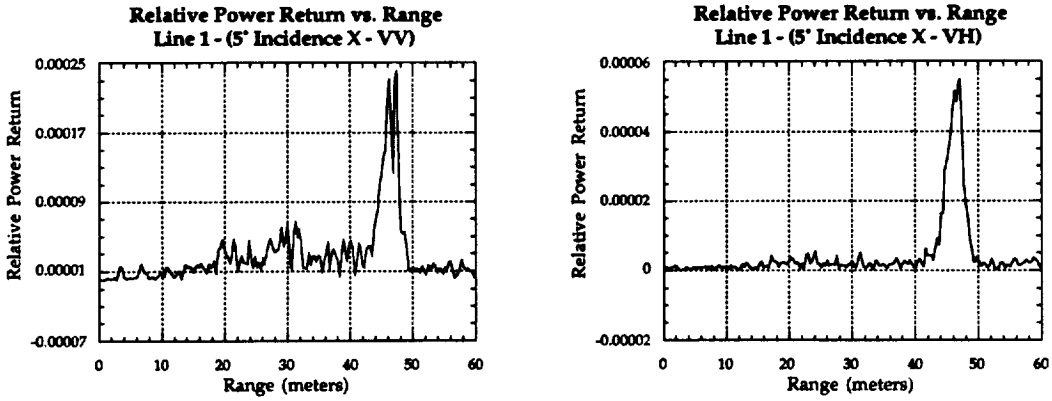

Figure 10. X-band returns from the Wallops experiment

6.0 Future Work

Over the next year we plan to concentrate on data processing and relating the data acquired to biophysical parameters. However, before intensive data processing begins, we will calibrate the radar at the NASA-GSFC antenna tower during July 1995 using a trihedral corner reflector and at The University of Kansas in August 1995 using a dihedral reflector. The trihedral reflector will allow us to measure the like-polarized response of the radar while the dihedral reflector will allow us to obtain the cross-polarized response of the radar.

We will begin the data processing effort by concentrating on the Wallops data set. Specifically, we will divide the forest into three layers and determine the relative contribution to the overall scattering from each of these layers. This will be done for each frequency band, polarization, and incidence angle. In addition, we will provide profiles of the scattering from the canopy as a function of range to the target and distance along the flight path.

We will then use allometry along with the data obtained by Dr. Jon Ranson to determine the biomass of different components within the forest. Using these data, we will perform a sensitivity study. This study will investigate the sensitivity of the radar data from the three canopy layers to the biomass of the corresponding layers. The results of this study will be used to determine which combination of frequency, polarization, and incidence angle is best for estimating the biomass of the different forest components. Additionally, we will use the scattering data to update and improve current microwave models used for forest canopies. This, in turn, can provide more accurate interpretation of SAR images of the forest.

We hope that the Wallops experiment will demonstrate the utility of further scatterometer experiments at the BOREAS SSA sites during the 1996 field campaigns. As a complement to the scatterometer data to be taken in 1996, we would like to collect data using a ground-based radar. The ground-based radar is an ultra-wideband network anlayzer system that sweeps from 2 to 18 GHz. This radar system has the ability to provide detailed information about the scattering from the forest floor and the other components of the forest understory.

7.0 Conclusions

We collected helicopter-borne scatterometer data at L, C, and X bands over the SSA sites during IFC-3. The data set collected is superior to that collected in IFC-2. However, further improvements to the radar were made after IFC-3. The results from IFC-3 show that at low incidence angles the L-band scatterometer can see the ground and that surface scattering is the dominant scattering mechanism at lower incidence angles. For C band, the ground